Egypt. J. of Appl. Sci., 34 (9) 2019 *194-213*

KINETIC ANALYSIS OF THE THERMAL DECOMPOSITION OF AMITRIPTYLINE HYDROCHLORIDE BY NONISOTHERMAL THERMOGRAVIMETRY

Laila Tosson Kamel*

Narcotic Department, National Centre for Social and Criminal Research
Zamalek , 11561, Cairo, Egypt

Key Words: Amitriptyline hydrochloride, isoconversional methods, DAEM method, master plots

ABSTRACT

The nonisothermal thermogravimetric decomposition of amitriptyline hydrochloride was investigated under pure nitrogen atmosphere at four different heating rates (β =5, 10, 15, 20^{o}C min^{-1}). Friedman, Flynn-wall-Ozawa, and Tang isoconversional methods were used to calculate the activation energy E_a. The results obtained was compared with that obtained by the distributed activation energy model, Miura procedure. Activation energy, E_a, results showed that the isoconversional kinetic methods used (Friedman, Flynn-Wall-Ozawa and Tang methods) were in good agreement with each other, together with the distributed activation energy model. It was found that the activation energy E_a was not really changed and was almost independent with respect to the level of conversion (α). This result suggests that the nonisothermal decomposition process of amitriptyline hydrochloride follows a single-step reaction. The master-plots were used to obtain the reaction kinetic model, which was confirmed by the integral composite I method. The kinetic triplet determined was, activation energy, E_a = 74.68 kJmol^{-1} , pre-exponential factor, A= 3.71×10^{3} min^{-1} and the reaction kinetic model follows the Avrami-Erofeev model, (nucleation and growth) , A4, $f(\alpha)= 4(1-\alpha)[-\ln(1-\alpha)]^{3/4}$, $g(\alpha) =[-\ln(1-\alpha)]^{1/4}$.

1- INTRODUCTION

Amitriptyline hydrochloride (AMT), with trade names**,** Vanatrip, Elavil, Endep, is an antidepressant drug under tricyclic antidepressant group. AMT has been widely used in the treatment of chronic pain, regardless of the presence of depression **(Burke et al.,2015).** It is used to treat many psychological disorder including major depressive disorder, anxiety, attention-deficit hyperactivity disorder, and bipolar disorder **(Dipalma and Katzung,1983).**

The thermal decomposition study, has received considerable attention all along the modern history, especially in the pharmaceutical field. Thermogravimetry, derivative thermogravimetry (TG/DTG) and differential thermal analysis (DTA), are analytic tools of high importance that helps in identifying the polymorphic forms, phase transitions, active–excipients

interactions, shelf life determinations, evaluation of the validity, thermal stability, products formed during decomposition, thermal decomposition kinetics and identification of drugs. **(Silva et al, (2015); Rodante et al (2002), Wang and You (2014); Salama et al (2015); Mohamed and Attia (2017) and Wang and You (2016))**

Thermal decomposition of AMT has important theoretical significance for further understanding its chemical properties. To our knowledge, the thermal decomposition of amitriptyline hydrochloride is not yet studied. In this paper the complete kinetic triplet of amitriplyline hydrochloride decomposition under nonisothermal conditions was calculated using multiple heating rates. Differential (Freidman method) and integral (Flynn Wall Ozawa and Tang methods), isoconversional (model-free) methods, mater plots and integral composite I method were used. The distributed activation energy model (DAEM) the Miura's procedure was also used for the investigation decomposition process.

2- EXPERIMENTAL

2.1. Materials

Amitriptyline hydrochloride (AMT) of at least 98% purity was purchased from Sigma Chemical Co. (St. Louis, MO, USA).

2.2. Instrument

The TG, DTG, and DTA curves were obtained by Shimadzu TGA-50 thermobalance, under nitrogen atmosphere gas at a flowing rate of 20 mL/min, at heating rates 5, 10, 15 and 20 °C min^{-1} with an average mass of samples, 3.584, 5.227, 5.445 and 5.496 mg, respectively, contained in an alumina crucible . Temperature range was from ambient one to 400°C.

3- Theoretical

The governing equation for kinetic analysis of solid state decomposition can be expressed as: $\frac{d\alpha}{dt} = K(T)f(\alpha)$ (1)

Where α is the degree of conversion and it increase from 0 to 1. $\alpha = \frac{m_o - m_t}{m_o - m_f}$

where, m_t represents the mass of the sample at time t (or temperature T), whereas m_o and m_f are the mass of the sample at the beginning and at the end of the process, respectively. T is the absolute temperature, K(T) represents the temperature – dependent rate constant, $\frac{d\alpha}{dt}$ is the conversion rate. $f(\alpha)$ is the differential conversion function (reaction model). The reaction models may take various analytical forms.

The temperature dependent rate constant is introduced by replacing K(T) with the Arrhenius equation, which gives

$$\frac{d\alpha}{dt} = A \exp\left(-\frac{E_a}{RT}\right) f(\alpha) \quad (2)$$

Where A is the pre-exponential (frequency) factor (min^{-1}), E_a is the apparent activation energy ($kJmol^{-1}$) and R is the gas constant (8.314 $kJmol^{-1}$).

For the nonisothermal measurement at constant heating rate of $\beta = dT/dt$ Eq. (2) may be transferred to

$$\frac{d\alpha}{dt} = \frac{A}{\beta} \exp\left(-\frac{E_a}{RT}\right) f(\alpha) \quad (3)$$

Equations (2 and 3) are the fundamental expressions of analytical methods to calculate kinetic parameters on the basis of TG data. Integration of eq. (3) leads to

$$g(\alpha) = \int_0^{\alpha} \frac{d\alpha}{f(\alpha)} = \frac{A}{\beta} \int_{T_o}^{T} \exp\left(-\frac{E_a}{RT}\right) dT \quad (4)$$

Where g(α) is the function of the reaction model in the integral form. and the right-hand side of Eq.(4) is a function known as the temperature integral that has no analytical solution but can be resolved either by numerical methods or by different approximations.

3.1. Isoconversional methods

The isoconversional methods are model independent that estimates the apparent activation energy at progressive degree of conversion by conducting multiple experiments at different constant heating rates are highly recommended for obtaining the reliable kinetic description of the investigated process. **(Jankovic and Mentus, 2009)**

In order to determine the apparent activation energy E_a and the pre exponential factor, ln A, the following methods are used.

3.1.1. Friedman method (FR) (Friedman,1964)

FR method, a linear differential isoconversional method based on Eq. (3) in the logarithmic form ,

$$\ln\frac{d\alpha}{dt} \equiv \ln\beta\frac{d\alpha}{dT} = \ln A\ f(\alpha) - \frac{E}{RT} \quad (5)$$

The apparent activation energy, E_a ,and the pre exponential factor ,lnA, are determined from the slope and intercept of the plot of ln(dα/dt) vs 1/T at a constant α value respectively.

3.1.2. Flynn–Wall–Ozawa method (FWO) (Flynn et al ,1966 and Ozawa ,1965)

FWO method, a linear integral method uses the following equation:

$$\ln\beta = \ln\frac{AE}{Rg(\alpha)} - 5.331 - 1.052\frac{E}{RT} \quad (6)$$

Plotting ln β vs 1/T should give straight lines, the slope of which is directly proportional to the activation energy and the intercept to the pre exponential factor lnA, at a constant α value .

3.1.3. Tang method (Tang, 2003)

Tang method, a linear integral method based on the following equation:

$$\ln\left(\frac{\beta}{T^{1.894661}}\right) = \ln\left(\frac{AE_a}{Rg(\alpha)}\right) + 3.635041 - 1.894661 \ln E_a - \frac{1.001450E_a}{RT} \quad (7)$$

Plotting $\ln\left(\frac{\beta}{T^{1.894661}}\right)$ vs 1/T should give straight lines, the slope of which is directly proportional to the activation energy and the intercept to the pre- exponential factor lnA, at a constant α value.

These plots are model independent since the estimation of the apparent activation energy does not require selection of particular kinetic model.

3.2- The Distributed Activation Energy model (DAEM) (Miura ,1995; Miura and Maki,1998)

Generally, the DAEM model may be written as the following expression

$$1 - \frac{V}{V^*} = \int_0^\infty exp\left(-A\int_0^{-1} e^{-\frac{E_a}{RT}}\,dt\right) f(E_a)dE_a \quad (8)$$

where a distribution function $f(E_a)$ is used to represent the difference in activation energies for an infinite number of irreversible first-order parallel reactions. *V* and *V** are the amount of volatile formed by time t, and the total volatile amount of the AMT sample, respectively.

Under linear non-isothermal conditions, Eq. (8) can be rewritten as follows:

$$\frac{V}{V^*} = 1 - \int_0^\infty exp\left(-\frac{A}{\beta}\int_0^{-1} e^{-\frac{E_a}{RT}}\,dT\right) f(E_a)dE_a = 1 - \int_0^\infty \varphi(E_a,T) f(E_a)dE_a \quad (9)$$

Where

$$\varphi(E_a,T) = \exp\left(-A\int_0^1 e^{\frac{-E_a}{RT}}\,dt\right) \cong exp\left(\frac{A}{\beta}\int_0^T e^{\frac{-E_a}{RT}}\,dt\right) \quad (10)$$

In the DAEM models, the activation energy function $f(E_a)$ can be conventionally described by a Gaussian distribution with a mean activation energy, E_0, and a standard deviation, σ.

$$f(E_a) = \frac{1}{\sigma\sqrt{2\pi}}\, exp\left[-\frac{(E_a - E_0)^2}{2\sigma^2}\right] \quad (11)$$

Recently, Miura and Maki **(Miura and Maki,1998)** have proposed a new simplified DAEM model. In their study, the temperature integral has been approximated with the following expression:

$$\int_0^T exp\left(-\frac{E_a}{RT}\right)dT \cong \left(\frac{RT^2}{E_a}\right) exp\left(-\frac{E_a}{RT}\right) \quad (12)$$

And with this approximation, the double exponential function φ(E_a ,T) becomes

$$\varphi(E_a,T) \cong exp\left(\frac{ART^2}{\beta E_a} e^{-\frac{E_a}{RT}}\right) \quad (13)$$

Further , the function φ(E_a , T) can be approximated by a step function at $E_a = E_s$ for a selected temperature T so that the activation energy E_s can be chosen to satisfy φ(E_a ,T) ≅ 0.58 using this approximation, Eq. (13) gives

$$0.545 .\frac{\beta E_a}{ART^2} = exp\left(-\frac{E_a}{RT}\right) \quad (14)$$

In the meantime, Eq. (9) can be simplified to

$$\frac{V}{V^*} \cong 1 - \int_{E_a}^{\infty} f(E_a)dE_a = \int_0^{E_a} f(E_a)dE_a \quad (15)$$

Obviously, this treatment approximates that only a reaction having E_a occurs at the specific temperature T and the heating rate β.

Finally, the related Arrhenius equation can be written as follows

$$\ln\left(\frac{\beta}{T^2}\right) = \ln\left(\frac{AR}{E_a}\right) + 0.6075 - \frac{E_a}{RT} \quad (16)$$

Thus, the Arrhenius plot of ln(β/T^2) versus 1/T at the same α conversion levels should be a straight line, and its slope and intercept can be used to determine the values of E_a and lnA, respectively. The activation energy distribution function *f*(E_a) can be obtained by differentiating the V/V* versus E_a relationship. In this method, the compensation effect between lnA and E_a was assumed to be ln A =ln a + bE_a ; and no assumption is required for the functional form of *f*(E_a). For simplicity, the symbol α, the degree of conversion, is used here for conversion in place of V/V*. The calculating procedure to estimate *f*(E_a) and A using the above-mentioned DAEM method, is given as follows:

(1) Obtain α versus T relationships at least three different heating rates;
(2) Calculate the values of ln(β/T^2) at selected a values for different heating rates;
(3) Plot ln(β/T^2) versus 1/T at selected α values, and determine the E_a and lnA values from the Arrhenius plots at different a values using Eq. (16);
(4) Plot the α versus E_a;
(5) Differentiate the α versus E_a relationship to obtain *f*(E_a).

3.3- Master Plots (Pedro et al, 2010)

The generalized kinetic equation introduced by **Ozawa, (1965)** was used for the proposal of universal master plots that were valid for

experimental data recorded under any heating profile. **(Gotor et al , 2000)**

Thus, if the generalized time is defined as**: (Ozawa, 1986)**

$$\theta = \int_0^t exp\left(\frac{-E}{RT}\right) dt \quad (17)$$

where, considering the integral of Eq. (2), it is clear that θ represents the time needed to reach a certain α value at infinite temperature. By differentiating Eq. (17) the following equation can be obtained:

$$\frac{d\theta}{dt} = exp\left(\frac{-E}{RT}\right) \quad (18)$$

The combination of eqs. (2 and 18) leads to

$$\frac{d\alpha}{d\theta} = Af(\alpha) \quad (19)$$

which can also be expressed in the following way:

$$\frac{d\alpha}{d\theta} = \frac{d\alpha}{dt}\ exp\left(\frac{-E}{RT}\right) \quad (20)$$

dα/dθ being the generalized reaction rate that, according to Eqs. (2, 19 and 20), represents the reaction rate extrapolated at infinite temperature as previously shown by **Ozawa, (1986)**. Since the previous knowledge of the activation energy allows for the extrapolation to infinite temperature of experimental data recorded under any heating profile, Eq. (20) should be valid for the analysis of any data, independently of the temperature profile under which they were obtained. From Eq. (19) and taking α = 0.5 as a reference we get:

$$\frac{d\alpha/d\theta}{(d\alpha/d\theta)_{0.5}} = \frac{f(\alpha)}{f(0.5)} \quad (21)$$

As *f*(0.5) is constant for a certain kinetic model, Eq. (21) indicates that for a given α, the reduced-generalized reaction rate, (dα/dθ)/(dα/dθ) α=0.5, would be equivalent to *f(*α*)/f(*0.5) when the proper *f*(α) is selected to describe the process. From Eq. (20 and 21), the relationship between the generalized reaction rate and the experimental data can be established:

$$\frac{d\alpha/d\theta}{(d\alpha/d\theta)_{0.5}} = \frac{d\alpha/dt}{(d\alpha/dt)_{0.5}}\ \frac{\exp(E/RT)}{\exp(E/RT)_{0.5}} \quad (22)$$

where $T_{0.5}$ represents the temperature corresponding to α = 0.5.

The previous knowledge of the activation energy is required in order to construct the experimental master plots. By plotting together the generalized reaction rate, as calculated from Eq. (22), and the fraction *f*(α)/*f*(0.5), corresponding to different theoretical kinetic models, versus α, it is possible to deduce by comparison the kinetic model followed by the process. Table (1) shows the algebric expressions for the most frequently used mechanisms of solid state process.

It must be noted that, according to Eq. (22), for non-isothermal experiments a single activation energy value is assumed. Therefore, for this analysis procedure to be valid, the studied process must obey single step kinetics. isoconversional analysis, must be used to check that the activation energy does not vary with α in a significant way.

Table (1) Algebric expression for the most frequently used mechanisms of solid state process

No	Mechanism	S*	Differential form $f(x)$	Integral form $g(x)$
Sigmoidal Curves (Nucleation and nuclei growth , Avrami-Erofeev equ.)				
1	N and G (n=1)	A1	(1-α)	$[-\ln(1-\alpha)]$
2	N and G (n=1.5)	A1.5	$(3/2)(1-\alpha)[-ln(1-\alpha)]^{1/3}$	$[-\ln(1-\alpha)]^{2/3}$
3	N and G (n=2)	A2	$2(1-\alpha)[-ln(1-\alpha)]^{1/2}$	$[-\ln(1-\alpha)]^{1/2}$
4	N and G (n=3)	A3	$3(1-\alpha)[-ln(1-\alpha)]^{2/3}$	$[-\ln(1-\alpha)]^{1/3}$
5	N and G (n=4)	A4	$4(1-\alpha)[-ln(1-\alpha)]^{3/4}$	$[-\ln(1-\alpha)]^{1/4}$
Deceleration curves				
6	Diffusion,1D	D1	$1/(2\alpha)$	α^2
7	Diffusion, 2D	D2	$1/-\left(ln(1-\alpha)\right)$	$(1-\alpha)ln(1-\alpha)+\alpha$
8	Diffusion,3D	D3	$1.5\left[(1-\alpha)^{-1/3}-1\right]$	$(1-2\alpha/3)-(1-\alpha)^{2/3}$
9	Diffusion,3D	D4	$\left[1.5(1-\alpha)^{2/3}\right]\left[1-(1-\alpha)^{1/3}\right]^{-1}$	$\left[1-(1-\alpha)^{1/3}\right]^2$
10	Diffusion,3D	D5	$(3/2)(1+\alpha)^{2/3}\left[(1+\alpha)^{1/3}-1\right]^{-1}$	$\left[(1+\alpha)^{1/3}-1\right]^2$
11	Diffusion,3D	D6	$(3/2)(1+\alpha)^{4/3}\left[1/(1+\alpha)^{1/3}-1\right]^{-1}$	$\left[1/(1+\alpha)^{1/3}-1\right]^2$
12	Contracted geometry shape (cylindrical symmetry)	R2	$2(1-\alpha)^{1/2}$	$1-(1-\alpha)^{1/2}$
13	Contracted geometry shape (sphere symmetry)	R3	$3(1-\alpha)^{2/3}$	$1-(1-\alpha)^{1/3}$
Acceleration curves				
14	power law (n=2)	P2	$2\alpha^{1/2}$	$\alpha^{1/2}$
15	power law (n=3)	P3	$3/2\alpha^{2/3}$	$\alpha^{1/3}$
16	power law (n=4)	P4	$4\alpha^{3/4}$	$\alpha^{1/4}$
17	power law (n=2/3)	P3/2	$2/3\alpha^{-1/2}$	$\alpha^{3/2}$
18	Mample power law (n=3/2)	P2/3	$3/2\alpha^{1/3}$	$\alpha^{2/3}$
19	Mample power law (n=4/3)	P3/4	$4/3\alpha^{-1/3}$	$\alpha^{3/4}$

4- RESULTS AND DISCUSSION

4.1- Characterization Results

The TG and DTG curves of the thermal decomposition process of AMT samples obtained at different heating rates (5, 10, 15, 20°C min^{-1}) under nitrogen atmosphere are shown in Figs (1 and 2) respectively. As shown in Fig. (1) TG curves are shifted to higher temperatures as the heating rates increases from 5 to 20°C min^{-1}. The shapes of the curves are quite similar, all curves showed one decomposition step. There is no mass loss up to 206°C, as temperature increases the TG curves exhibit a total mass loss in the temperature range 274.47-327.97°C. Fig. (2) shows the DTG peaks of the thermal decomposition of AMT. Peaks become stronger and wider as the heating rate increases from 5 to 20°Cmin^{-1} and the peak temperature is promoted from 242.15 to 281.72°C.

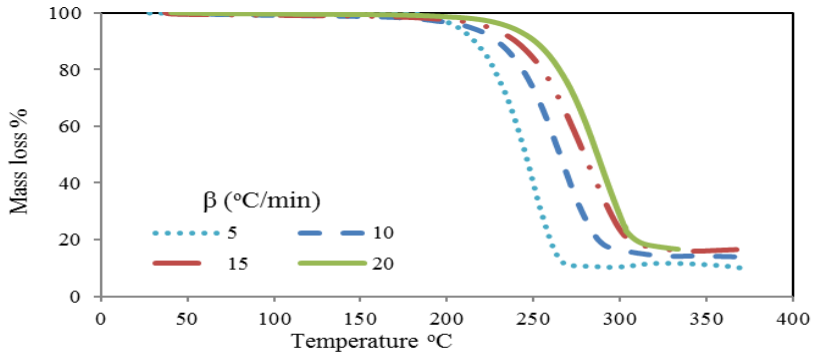

Fig.(1) TG curves for the thermal decomposition of AMTin nitrogen atomsphere at different heating rates (5, 10, 15, and 20°Cmin^{-1})

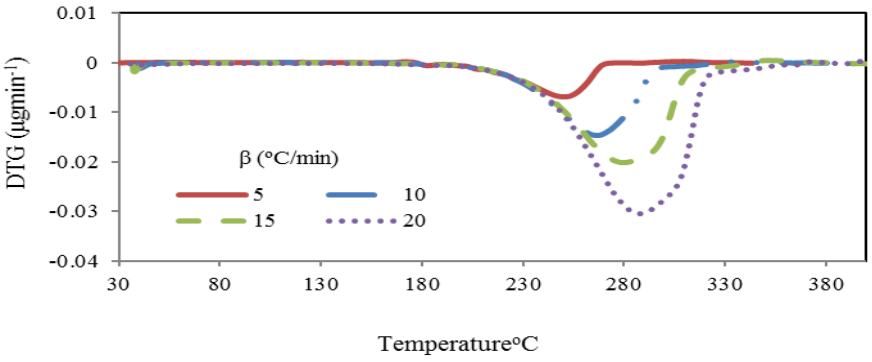

Fig.(2) DTG curves for the thermal decomposition of AMT in nitrogen atmosphere at different heating rates (5, 10, 15, 20°Cmin^{-1})

It is evident from both curves (TG/DTG) that the thermal decomposition of AMT exhibited only one single step reaction. Fig. (3) shows the DTA curve of AMT at $10^{o}C\ min^{-1}$. The curve presents a first strong peak at $198^{o}C$, which corresponds to the melting process of the AMT. The second broad peak, in the temperature range $289\text{-}320^{o}C$, shows the endothermic nature, of the decomposition process.

Amitriptyline hydrochloride (AMT), (3-(10,11-dihydro-5H-dibenzo [*a*,*d*]cycloheptane-5-ylidene)-N,N-dimethyl-1-1-propanamine), has a dibenzocycloheptadiene structure with rigid, almost planar tricyclic ring system and a short hydrocarbon chain carrying a terminal nitrogen atom attached to cycloheptadiene through methylene groups with an exocyclic double bond substituted with N,N-dimethyl 1,1 propane amino side chain. The structure of amitriptyline is shown in Fig.(4).

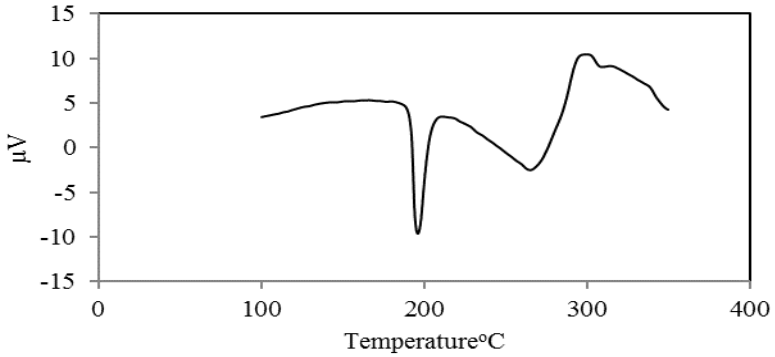

Fig.(3) DTA curve for the thermal decompostion of AMT in nitrogen atmosphere at $10^{o}Cmin^{-1}$

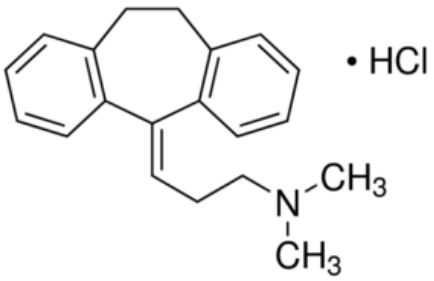

Fig.(4) The structure of AMT

Thermal decomposition of organic molecules is due to the molecular kinetic energy increasing during heating. These include atomic oscillations that rupture the weaker chemical bonds. The fragmentation of tricyclic antidepressants is similar to that of phenothiazines **(Kollroser**

and Schober , 2002). Fig.(5) shows the proposed mechanism of the thermal decomposition of AMT. The bond between the tricyclic ring and the dimethylamine group in the side chain is broken, which results in the formation of iminium ion $(H_2C=N(CH_3)_2)^+$ with complete decomposition in one step.

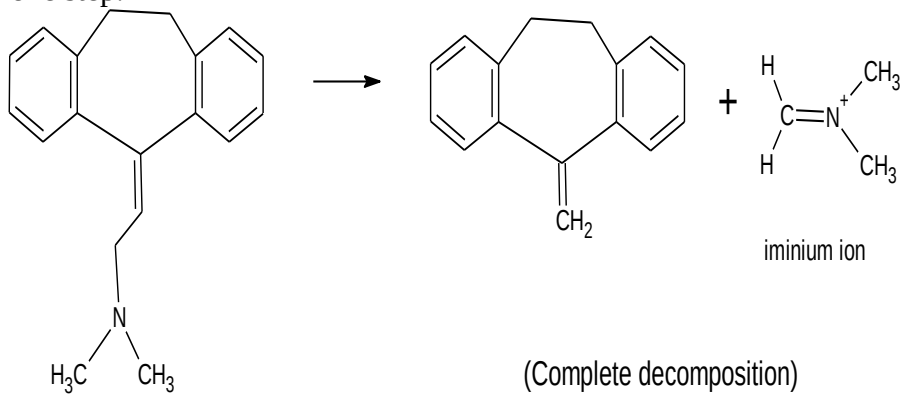

Fig.(5) The proposed mechanism of the thermal decomposition of AMT

4.2. - Calculation of Activation Energy E_a

4.2.1- Isoconversional methods

The conversion values, α, range from ($0.2 \leq \alpha \leq 0.8$) were used in this work rather than the entire range. This range is strongly recommended because solid-state reactions are not stable at the beginning and ending periods. Solid-state reaction usually contains a diffusion process **(Koga and Criado 1998a&b)**, as it generates temperature and partial pressure gradient. Consequently, it generates reaction gradient from the outer to the inner surface of the solid sample. As a result, the real activation energy values at this period are different from the ones at the middle period (0.2 to around 0.8). **(Jankovic et al, 2009)**

Figs (6, 7 and 8) show a typical FR , FWO and Tang isoconversional methods plots which are constructed according to eq. (5, 6, 7) respectively to evaluate the slopes of ln (dα/dt) *vs*. 1/T , ln (β/T^2) *vs*. 1/T and $ln\left(\frac{\beta}{T^{1.894661}}\right)$ vs 1/T respectively . Figs. (6, 7 and 8) show that the conversional lines at all considered conversion levels have almost the same slopes . The apparent activation energy was determined:

(FR) $E_{a,\ FR}$ = 70.24 kJmol^{-1} , (FWO) $E_{a,FWO}$ = 78.61kJmol^{-1} , (Tang), $E_{a,Tang}$ = 75.12 kJmol^{-1} .

It should be noted that these results are obtained without any knowledge of the reaction model function.

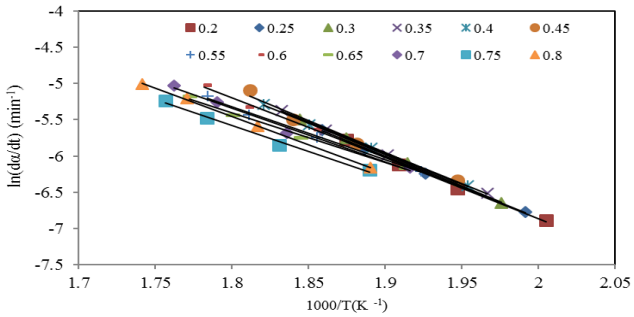

Fig. (6) Arrhenius plots of ln(dα/dt) versus 1000/T at chosen α values (FR method)

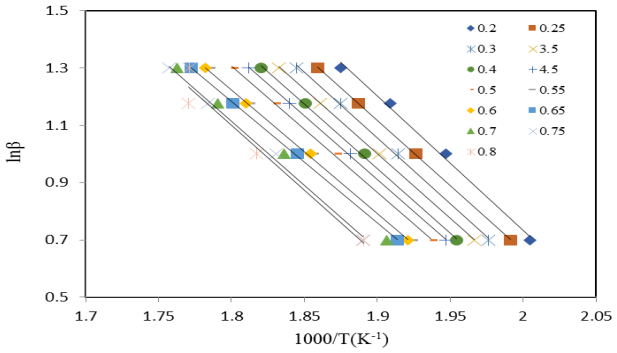

Fig.(7) Arrhenius plots of lnβ versus 1000/T at chosen α values (FWO method)

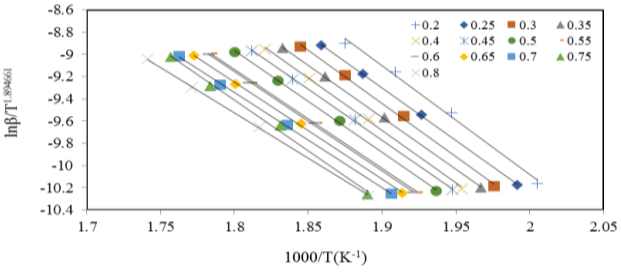

Fig.(8) Arrhenius plots of ln β/T$^{1.894661}$versus 1000/T at chosen α values (Tang method)

4.2.2. The distributed activation energy model (DAEM)

The Arrhenius plot of ln(β/T^2) vs 1/T at the same α conversion levels was constructed according to eq. (16) is shown in Fig. (9). All lines have almost the same slopes, the apparent activation energy was determined (DAEM) $E_{a,\ DAEM}$ = 74.76 kJmol^{-1}.

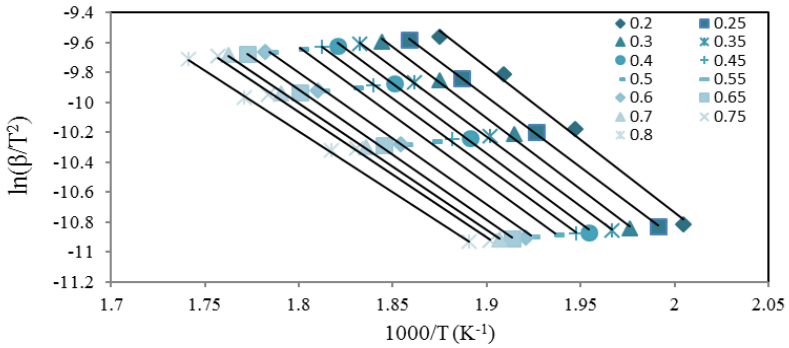

Fig.(9) Arrhenius plots of $\ln\beta/T^2$ versus 1000/T at chosen α values (DAEM method)

It is clear that the apparent activation energy E_a values calculated using different methods are in good agreement with each other. It is observed that the value of E_a calculated by means of FR method is slightly lower than those calculated by means of (Tang and FWO) methods, and the DAEM method. It is also shown that the E_a determined by FWO is slightly higher. These differences may be attributed to different ways to derive the relations being the back ground of these methods. Kinetic parameters of thermal decomposition of AMT corresponding to different degrees of conversion α calculated by Freidman (FR), Flynn Wall Ozawa (FWO), Tang and DAEM equations respectively are shown in Table (2). The dependence of the apparent activation energy E_a on the extent of conversion, α, (E_a-α plot) **(Budrugeac et al, 2001a&b; Sbirrazuoli et al, 1997)** for the nonisothermal decomposition process of AMT is shown in Fig. (10). It is observed that regardless of the calculation procedure used the activation energy E_a remain partially constant ie. does not depend on α, the relative error is less than 6%. This suggests that the nonisothermal decomposition process of AMT follows a single step reaction.

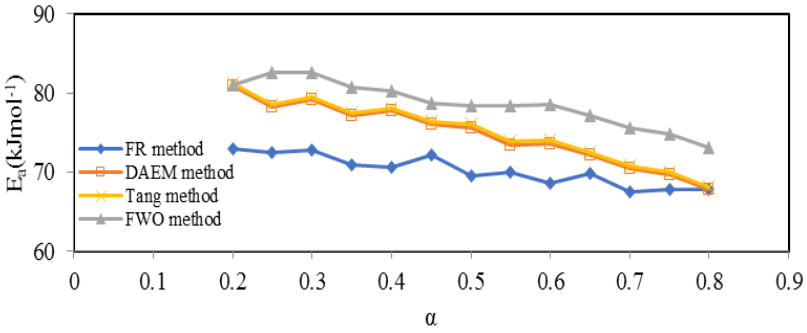

Fig.(10) Dependence of E_a on α ($0.2 \leq \alpha \leq 0.8$) for the thermal decomposition of AMT

Table (2) The E_a and lnA values of thermal decomposition of AMT corresponding to different degrees of conversion α

	FR method			FWO method			Tang method			DAEM method		
α	E_a	lnA	R^2	E_a	lnA	R^2	E_a	lnA	R^2	E_a	lnA	R^2
0.2	72.92	9.08	0.996	81.02	10.19	0.993	81.18	8.69	0.995	80.84	10.38	0.995
0.25	72.56	9.19	0.999	82.65	9.89	0.999	78.62	7.87	0.999	78.28	9.56	0.999
0.3	72.78	9.37	1	82.59	10.38	0.998	79.55	7.95	0.993	79.2	9.64	0.993
0.35	70.86	8.77	0.998	80.68	10.15	0.999	77.49	7.34	0.999	77.14	9.02	0.999
0.4	70.67	8.417	0.999	80.31	10.16	0.999	78.10	7.36	0.998	77.75	9.05	0.998
0.45	72.23	9.19	0.980	78.67	9.50	0.998	76.34	6.85	0.999	75.99	8.53	0.999
0.5	69.45	8.34	0.995	78.38	9.90	0.999	76.00	6.66	0.999	75.64	8.34	0.999
0.55	69.99	7.99	0.993	78.38	9.65	0.999	73.83	6.00	0.998	73.46	7.67	0.998
0.6	68.54	8.08	0.987	78.52	9.65	0.999	73.96	6.01	0.999	73.6	7.68	0.997
0.65	69.85	8.45	0.991	77.23	9.52	0.999	72.56	5.59	0.999	72.19	7.27	0.999
0.7	67.56	7.58	0.987	75.59	9.32	0.999	70.80	5.10	0.999	70.43	6.77	0.999
0.75	67.86	7.88	0.991	74.83	9.23	0.999	69.99	4.86	0.999	69.61	6.52	0.995
0.8	67.84	7.48	0.999	73.12	9.03	0.995	68.12	4.30	0.999	67.74	5.96	0.999
Av	70.24	8.45		78.61	9.73		75.12	6.51		74.76	8.18	

4.3. Determination of the most probable reaction mechanism

Master plots are reference theoretical curves that depend on the kinetic model but are independent of the kinetic parameters. Experimental data can easily be transformed into experimental master plots and compared with the theoretical ones determined for the different kinetic models. Comparing various kinetic models with the experimental master plot, the appropriate kinetic model can be easily selected.

Fig.(11) shows the comparison between the master plots constructed from the experimental data eq. (22) at the four heating rates (5, 10, 15, 20^{o}Cmin^{-1}) using the average value of the apparent activation energy E_a (74.68kJ mol^{-1}) in conversion fraction, α, ($0.20 \leq \alpha \leq 0.80$) with the plots constructed from the most usual kinetic models Table (1). It is clear that the thermal decomposition of AMT has a very close resemblance to the nucleation and growth kinetic models, Avrami-Erofeev model, A4, $f(\alpha)= 4(1-\alpha)[-\ln(1-\alpha)]^{3/4}$, $g(\alpha) =[-\ln(1-\alpha)]^{1/4}$.

The observed displacement of the curve is attributed to the difference between the real process and the ideal conditions.

In order to confirm the established reaction mechanism, the integral I composite method, was applied. The composite method presuppose one single set of activation parameters for all conversions and heating rates. In this way, all the experimental data can be superimposed in one single master curve.

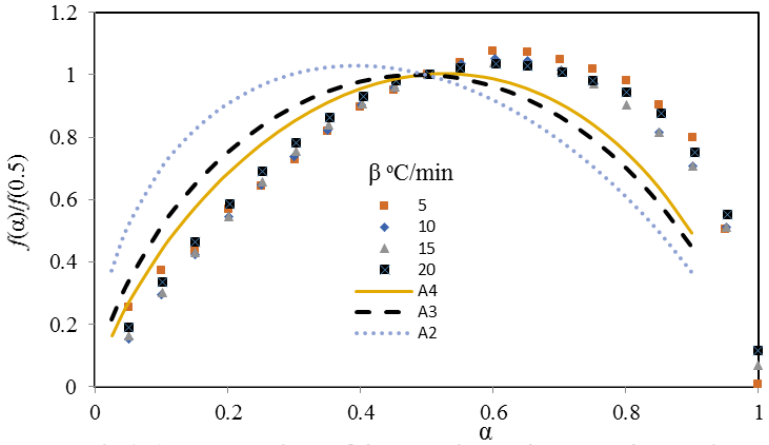

Fig.(11) A comparison of the experimental master plots against α for the thermal decomposition of AMT with the theoretical master curves of *f*(α)/*f(0.5*) against α

The composite integral method I **(Budrugeac and Segal, 2005; Gabal, 2003)** is based on the Coats–Redfern equation **(Coats and Redfern , 1964)** which is rewritten as follows:

$$\ln\left(\beta\frac{g(\alpha)}{T^2}\right)=\ln\left(\frac{AR}{E_a}\right)-\frac{E_a}{RT}$$

For each form of g(α), the curve $\ln\left(\beta\frac{g(\alpha)}{T^2}\right)$ vs 1/T was plotted for the experimental data obtained at different heating rates. The kinetic model that gives the best correlation coefficient where the data falls in a single master straight line is chosen.

From Fig.(12), it is clear that A4 model, $f(\alpha)= 4(1-\alpha)[-\ln(1-\alpha)]^{3/4}$, $g(\alpha) =[-\ln(1-\alpha)]^{1/4}$, best fits the decomposition process because all the different heating rate data are in only one master curve.

4.4. Calculation of pre-exponential factor

The pre-exponential factor lnA is estimated from the intercepts of the plots of Figs (6, 7, 8), by inserting the obtained most probable kinetic function model, A4, in the eqs. (5,6,7. $f(\alpha)$ $4(1-\alpha)((-\ln(1-\alpha))^{3/4}$ was inserted in eq.(5),where the $g(\alpha) =[-\ln(1-\alpha)]^{1/4}$ was inserted in eqs. (6 and 7). Results show that the pre-exponential factor ,A, values range from 10^3 to 10^4 min^{-1} and the average value of ,A, is $3.71 \times 10^3 min^{-1}$.

Fig. (13) shows the functional dependence between lnA and E_a of AMT. The linear relationship between lnA and activation energy E_a could possibly be written as

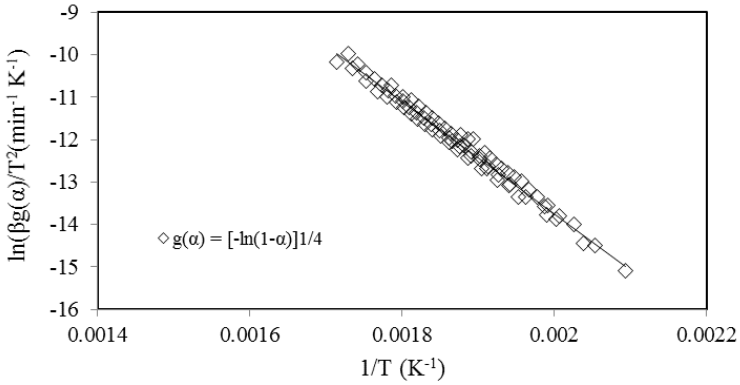

Fig.(12) Composite integral I of nonisothermal TG data
(5, 10, 15, and 20°C min^{-1})

lnA = 0.3085E_a -13.136. lnA versus E_a relationship indicates that there is a kinetic compensation effect, that is to say, there exist a compensatory increase of lnA with an increasing activation energy E_a. The kinetics compensation effect is due to the change in reactant properties during the sample decomposition reaction, which becomes more difficult to occur as the conversion increases, subsequently presenting a higher activation energy **(Zhen H. et al, 2015)**. Obviously, the pre exponential factor lnA is not a constant because of the change in the reacted component

4.5 Miura –Maki DAEM model

The distributed activation energy model (DAEM) is applied to study the thermal decomposition kinetics. According to eq. (16), a new simple method was used. The E_a and A values of thermal decomposition of the AMT corresponding to different degrees of conversion α are obtained simultaneously. Results are shown in Table 2.

The variation of the pre-exponential factor lnA with activation energy E_a is given in Fig. (13). A functional dependence between the pre-exponential factor, lnA, with activation energy, E_a , can be obtained as the following empirical equation: lnA =0.3349E_a – 18.603

The distribution curve $f(E_a)$ for AMT decomposition is obtained by differentiating α with respect to E_a and the results are shown in Fig.(14). It can be observed from the Fig.(14) that the estimated curve for the investigated process represents a sharp peak and does not show a broad peak and the apparent activation energy does not spread in the large E_a interval. The peak position is placed in a single point at E_a =

73.45kJ/mol. It can be pointed out that the value of E_a is very similar to the value of E_a calculated by the isoconversional methods.

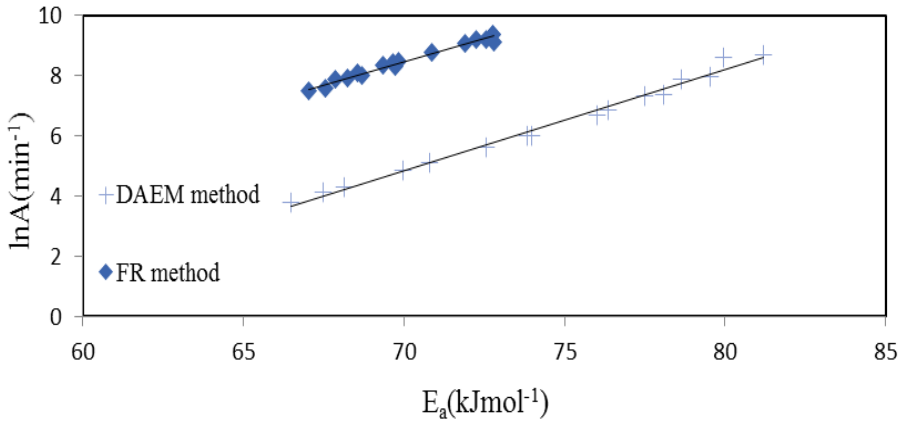

Fig.(13) Dependence of lnA on E_a of the thermal deomposition of AMT

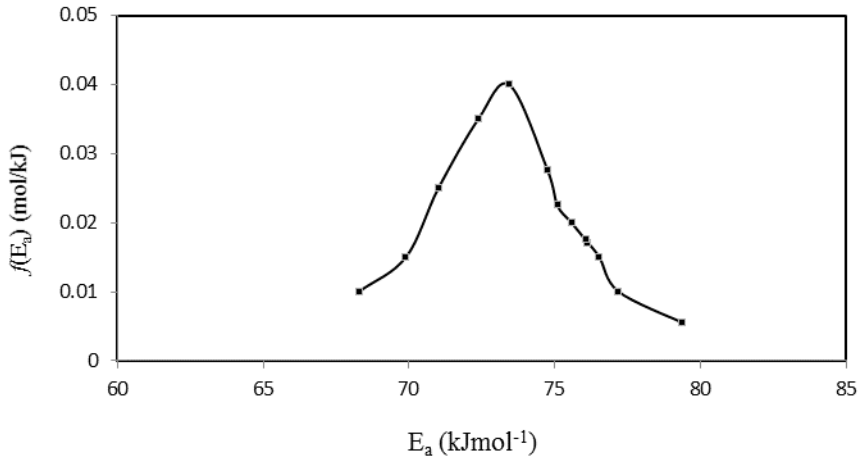

Fig. (14) The activation energy distribution function $f(E_a)$ curves obtained using DAEM method

CONCLUSION

The kinetics of the nonisothermal decomposition of AMT was accurately determined from a series of thermo analytical experiments at four constant heating rates (5, 10, 15, 20^{o}Cmin^{-1}). The apparent activation energy (E_a) was calculated by the differential isoconversional

(Friedman) and integral isoconversional (FWO and Tang) methods without a previous assumption of the kinetic model of the reaction.

It was found that:

- The apparent activation energy ,E_a , was not really changed and was nearly independent with respect to the level of conversion (α). This suggests that the nonisothermal decomposition process of AMT follows a single-step reaction.
- The master plots method was used to define the most probable mechanism, $f(\alpha)$, for the investigated decomposition process. From the obtained results, it was found that the most probable reaction mechanism belongs to the mechanism of the nucleation and growth kinetic models , Avrami-Erofeev model, A4, $f(\alpha)= 4(1-\alpha)[-\ln(1-\alpha)]^{3/4}$, $g(\alpha) =[-\ln(1-\alpha)]^{1/4}$, the integral I composite method, was applied to confirm the established reaction mechanism.
- Miura procedure, (DAEM) was applied, the experimental distribution curve of the apparent activation energies, $f(E_a)$, was estimated. The value of E_a determined was very similar to that calculated by the isoconversional methods.
- As a final conclusion ,the kinetic triplet of the nonisothermal thermogravimetric decomposition of amitriptyline hydrochloride was ,E_a = 74.68 kJmol^{-1} , A= 3.71×10^3 min^{-1} (ln A= 8.22), reaction model follows the Avrami-Erofeev model, A4, $f(\alpha)= 4(1-\alpha)[-\ln(1-\alpha)]^{3/4}$, $g(\alpha) =[-\ln(1-\alpha)]^{1/4}$, (nucleation and growth) .

REFERENCES

Budrugeac, P. and E. Segal (2005): On the use of Diefallah's composite integral method for the non-isothermal kinetic analysis of heterogeneous solid-gas reactions, J. Therm. Anal. Calorim., 82: 677–680.

Budrugeac, P. ; D.Homentcovschi and E. Segal (2001a): Critical analysis of the isoconversional methods for evaluating the activation energy. I, Theoretical background J Therm Anal Calorim, 63: 457–463.

Budrugeac, P.; D. Homentcovschi and E. Segal, (2001b): Critical considerations on the isoconversional methods. III, On the evaluation of the activation energy from non-isothermal data, J Therm Anal Calorim., 66: 557–565

Burke, N.N. ; D.P. Finn and M. Roche (2015): Chronic administration of amitriptyline differentially alters neuropathic pain-related

behaviour in the presence and absence of a depressive-like phenotype, Behav. Brain Res., 278: 193–201.

Coats, A.W. and J.P. Redfern (1964): Kinetic Parameters from Thermogravimetric Data, Nature, 201, 68-69.

Dipalma, J.R. and B.G. Katzung (1983): Basic clinical pharmacology, Am Fam Physician, 28: 393.

Flynn, J.H. and L.A. Wall (1966): General treatment of the thermogravimetry of polymers. Journal of Research of the National Bureau of Standards, 70A: 487-523.

Friedman, H.L. (1964): Kinetic of thermal degradation of char-forming plastics from thermogravometry, J. Polym. Sci. Part C, 6: 183-195.

Gabal, M.A. (2003): Kinetics of the thermal decomposition of CuC_2O_4–ZnC_2O_4 mixture in air, Thermochim. Acta, 402: 199–208.

Gotor, F.J.; J.M. Criado; J. Malek and N. Koga (2000): Kinetic analysis of solid-state reactions: The universality of master plots for analyzing isothermal and nonisothermal experiments, J. Phys. Chem. A, 104:10777-10782.

Jankovic, B. and S. Mentus (2009): A kinetic study of the nonisothermal decomposition of palladium acetylacetonate investigated by thermogravimetric and X-Ray diffraction analysis determination of distributed reactivity model metallurgical and materials, Transactions A ,40A: 609-624.

Jankovic, B. ; S. Mentus and D. Jelic (2009): A kinetic study of non-isothermal decomposition process of anhydrous nickel nitrate under air atmosphere, Physica B, 404: 2263–2269.

Koga, N. and J.M. Criado (1998a): The influence of mass transfer phenomena on the kinetic analysis for the thermal decomposition of calcium carbonate by constant rate thermal analysis (CRTA) under vacuumInt. J. Chem. Kinet., 30, 737–744.

Koga, N. and J.M. Criado (1998b): Kinetic Analyses of Solid-State Reactions with a Particle-Size Distribution, J. Am. Ceram. Soc., 81: 2901–2909.

Kollroser, M. and C. Schober (2002): Simultaneous determination of seven tricyclic antidepressant drugs in human plasma by direct-injection HPLC-APCI-MS–MS with an ion trap detector, Therapeutic Drug Monitoring, 24: 537–544.

Miura, K. (1995): A new and simple method to estimate *f*(E) and k_o(E)in the distributed activation energy model from three sets of experimental data, Energy and Fuels., 9: 302–307.

Miura, K. and T. Maki (1998): A simple method for estimating *f*(E) and k_o(E)in the distributed Activation energy model Energy, Energy and Fuels, 12: 864–869.

Mohamed, M. and A. Attia (2017): Thermal behavior and decomposition kinetics of cinnarizine under isothermal and non-isothermal conditions. Therm Anal Calorim., 127: 1751–1756.

Ozawa, T. (1965): A new method of analyzing thermogravimetric data, Bull Chem Soc Jpn.; 38: 1881–1886.

Ozawa, T. (1986): Non-isothermal kinetics and generalized time, Thermochim. Acta., 100: 109-118.

Pedro, E. ; A. Pérez-Maqueda ; A. Perejón and J. Criado (2010): Generalized kinetic master plots for the thermal degradation of polymers following a random scission sechanism, J. Phys. Chem. A, 114: 7868–7876.

Rodante, F.; S. Vecchio and M. Tomassetti (2002): Kinetic analysis of thermal decomposition for penicillin sodium salts model-fitting and model-free methods, Journal of Pharmaceutical and Biomedical Analysis, 29: 1031–1043.

Salama, N.; M. Mohammad and T. Fattah (2015): Thermal behavior study and decomposition kinetics of amisulpride under non-isothermal and isothermal conditions, J Therm Anal Calorim, 120: 953–958.

Sbirrazuoli, N.; Y. Girault and E. Elegant (1997): Simulations for evaluation of kinetic methods in differential scanning calorimetry. Part 3 — Peak maximum evolution methods and isoconversional methods, Thermochim Acta., 293: 25–37 .

Silva, A.C.M.; D.A. Gálico ; R.B. Guerra; G.L. Perpétuo; A.O. Legendre ; D. Rinaldo and G.Bannach (2015): Thermal stability and thermal decomposition of the antihypertensive drug amlodipine besylate, J Therm Anal Calorim., 120: 889–92.

Tang W.J.; Y.W Liu.; H. Zhang and C.X. Wang (2003): New approximate formula for Arrhenius temperature integral, Thermochimica Acta, 408: 39-43.

Wang, X. and J.You (2014): The mechanism and kinetics of the thermal decomposition of telbivudine, Journal of Analytical and Applied Pyrolysis, 108: 228–233.

Wang, X. and J. You (2016): Study on the thermal decomposition of capecitabine, J Therm Anal Calorim., 123: 2485–2497.

Zhen, H.; Y.Qiao-qiao and T. Li-jun (2015): A comparison study on thermal decomposition behavior of poly (L-lactide) with different kinetic models, J Therm Anal Calorim, 119, 2015–2027.

التحليل الحراري الحركي لهيدروكلوريد أميتريبتيلين بواسطة القياس الحراري غير المتساوي

ليلى طوسون كامل

المركز القومى للبحوث الاجتماعية والجنائية

قسم بحوث المخدرات

اميبرامين هيدروكلوريد و الذى له الاسماء التجارية ، Vanatrip، Elavil، Endep ، هو دواء مضاد للاكتئاب ضمن مجموعة مضادات للاكتئاب ثلاثية الحلقة. يستخدم الاميبرامين هيدروكلوريد على نطاق واسع فى علاج الألم المزمن ، بغض النظر عن وجود الاكتئاب. كما يتم استخدامه لعلاج العديد من الاضطرابات النفسية بما في ذلك اضطراب الاكتئاب الشديد والقلق واضطراب فرط النشاط .تهدف الدراسة الى حساب الثبات الحراري و التعرف على المركبات الناتجة أثناء التحلل لحرارى فى درجات عالية كذلك حركيات التحلل الحراري .تفيد هذه الدراسة فى تحسين جودة تصنيع هذا العقار فى المستقبل و معرفة درجات الحرارة المثالية لتخزين العقار.

تم قياس التحلل الحراري لهيدروكلوريد أميتريبتيلين في جو نيتروجين نقي بأربعة معدلات تسخين مختلفة 5و10و15و20 درجة مئوية فى الدقيقة . استخدمت طرق فريدمان وفلن وول اوزاوا وتانج في حساب طاقة التنشيط . و كذلك طريقة نموذج طاقة التنشيط الموزع لحساب الطاقة التنشيط. أظهرت النتائج ان طاقة التنشيط ، E_a المحسوبة، بالطرق الحركية المتناظرة المستخدمة (طرق فريدمان و فلن وول أوزاوا و تانج) في اتفاق جيد مع بعضها البعض ، جنبا إلى جنب مع نموذج طاقة التنشيط الموزعة. وقد تبين أن طاقة التنشيط E_a لم تتغير وكانت مستقلة فيما يتعلق بمستوى (α). هذه النتيجة تشير إلى أن عملية التحلل الحرارى هيدروكلوريد لأميتريبتيلين تم فى خطوة واحدة. تم استخدام master plots للحصول على نموذج التفاعل الحركي ، والذي تم تأكيده بواسطة طريقة المركب I المتكاملة. اظهرت النتائج ان ، طاقة التنشيط ، mol/Ea = 74.68 kJ ، عامل ما قبل الأس ، A = 3.71×10^3 دقيقة$^{-1}$ ونموذج التفاعل الحركي يتبع نموذج Avrami-Erofeev . (النواة والنمو).